Respiratory Research

RESEARCH

Open Access

Ivacaftor ameliorates mucus burden, bacterial load, and inflammation in acute but not chronic *P. aeruginosa* infection in hG551D rats

Johnathan D. Keith[1], Mikayla Murphree-Terry[1,2], Gretchen Bollar[1,2], Ashley M. Oden[2], Ian H. Doty[2] and Susan E. Birket[1,2*]

Abstract

Background Newly approved highly effective modulation therapies (HEMT) have been life-changing for people with CF. Although these drugs have resulted in significant improvements in lung function and exacerbation rate, bacterial populations in the lung have not been eradicated. The mechanisms behind the continued colonization are not completely clear.

Methods We used a humanized rat to assess the effects of ivacaftor therapy on infection outcomes. Rats harbor an insert expressing humanized CFTR cDNA, including the G551D mutation. hG551D rats were treated with ivacaftor either during or before infection with *P. aeruginosa*. The response to infection was assessed by bacterial burden in the lung and mucus burden in the lung.

Results We found that hG551D rats treated with ivacaftor had reduced bacteria present in the lung in the acute phase of the infection but were not different than vehicle control in the chronic phase of the infection. Similarly, the percentage of neutrophils in the airways were reduced at the acute, but not chronic, timepoints. Overall weight data indicated that the hG551D rats had significantly better weight recovery during the course of infection when treated with ivacaftor. Potentiation of the G551D mutation with ivacaftor resultant in short-circuit current measurements equal to WT, even during the chronic phase of the infection. Despite the persistent infection, hG551D rats treated with ivacaftor had fewer airways with mucus plugs during the chronic infection.

Conclusions The data indicate that the hG551D rats have better outcomes during infection when treated with ivacaftor compared to the vehicle group. Rats have increased weight gain, increased CFTR protein function, and decreased mucus accumulation, despite the persistence of infection and inflammation. These data suggest that ivacaftor improves tolerance of infection, rather than eradication, in this rat model.

*Correspondence:
Susan E. Birket
susanbirket@uabmc.edu
[1] Gregory Fleming James Cystic Fibrosis Research Center, University of Alabama at Birmingham, 1720 2nd Ave S, Birmingham, AL 35294, USA
[2] Division of Pulmonary, Allergy, and Critical Care, Department of Medicine, University of Alabama at Birmingham, Birmingham, AL, USA

Introduction

In 2011, the FDA approved the first small molecule therapeutic that targets the basic defect of cystic fibrosis [1]. Ivacaftor potentiates the cystic fibrosis transmembrane conductance regulator (CFTR) protein, by

improving gating in the G551D mutation [2, 3]. It has since been approved for a handful of other mutations, and has been combined with small molecules to correct the protein folding defect that occurs with mutations like F508del [4–8]. These drugs have now reached a significant portion of the patient population in the United States and Europe, and have made dramatic changes in the overall health and quality of life for those who are eligible [9–12]. Together, these drugs have been referred to as highly effective modulator therapies, or HEMT, and have been proven in the clinic to improve sweat chloride [13, 14], lung function [15], mucociliary clearance [16], nutritional status [17], and to reduce pulmonary exacerbations [18].

Early data from the GOAL study, which collected data on subjects with ivacaftor therapy for up to a year after initiation, indicated early promising results on infectious outcomes [19]. Specifically, the GOAL study found that ivacaftor cause a reduction in the incidence of *Pseudomonas aeruginosa* infection, within a few months of therapy onset, although most other pathogens were unchanged. However, follow-up data, and corroborating studies from Europe, indicated that these changes were short lived [20]. The recently released PROMISE data set also showed promising signs of reduced exacerbations in subjects eligible for Trikafta [12], but also found that infection largely persisted in the lung. It is not clear why the bacteria remain, or how impactful future infections will be to patients' health [11].

In order to address these questions in a more controllable animal model of CF, we created a humanized rat model that expresses CFTR with a G551D mutation [21]. We have previously shown that this model responds to ivacaftor with approximately 50% of the function of WT CFTR, that ivacaftor is able to restore mucociliary transport and airway hydration, and also that ivacaftor incompletely restores inflammatory outcomes when the animal is challenged to mimic an exacerbation [22]. In this study, we extended the evaluation of ivacaftor to understand how the restoration of CFTR results alters infection.

The hG551D model of CF replicates both the mucoobstructive and chronic infection phenotype seen previously in CF rat models [23–25], which more faithfully represents lung disease of human subjects. This rat also offers a proxy model for restoration of CFTR by any means, enabling questions regarding the extent of CFTR activity necessary to correct specific aspects of pathophysiology. This is a method that has been used in other animal models [26, 27], and enables us to understand the relationship between airway mucus, *P. aeruginosa* infection, and CFTR activity.

In the study presented here, we examined the effects of ivacaftor on either treating or preventing infection with *P. aeruginosa*, how mucus accumulation following infection was affected by ivacaftor, and how CFTR potentiation was changed during infection, to understand the molecular effects of ivacaftor therapy during acute and chronic lung infection.

Materials and methods

CF rat model

Experiments were conducted using the humanized-G551D-CFTR strain [21] either homozygous G551D (termed hG551D) or their littermate controls without the G551D insert (termed WT). This strain was bred and genotyped as previously described [28]. Heterozygote (CFTR hG551D/+) male and female were paired to generate WT and hG551D pups, as above. All animals were bred and housed in standard cages maintained on a 12 h light/dark cycle with ad libitum access to food and water, in temperatures ranging from 71 to 75°F. hG551D and WT animals were maintained on a standard rodent diet with supplemental DietGel 76A (clear H20, Westbrook, ME, United States) and a combination of PEG3350 (Spectrum Chemical, New Brunswick, NJ, United States), Pedialyte Advanced Care Plus Powder (Abbott, Abbot Park, IL, United States), and sodium benzoate (Sigma-Aldrich) added to the water from weaning, as a means to reduce mortality from gastrointestinal obstruction. Studies were conducted at 6 months of age. Groups were split as evenly as possible between males and females.

Pharmacologic administration

WT and hG551D rats received administration of ivacaftor, obtained from Selleckchem (Houston, TX, United States), and suspended in methylcellulose. Ivacaftor was mixed with methylcellulose no more than 3 days prior to administration and stored at 4 °C. Experiments followed different schedules of administration, but all animals either received ivacaftor at a rate of 30 mg/kg/day or 3% methylcellulose vehicle by oral gavage.

Pseudomonas aeruginosa

Rats were infected with the mucoid *P. aeruginosa* strain PAM57-15, a clinical isolate used previously [24, 29]. Bacteria were grown in tryptic soy broth (TSB) to absorbance of 1.0–1.5 at 600 nm and washed in PBS, pH 7. Bacteria were embedded in agarose using previously established methods and adjusted to a concentration of 1×10^6 CFU/mL. In order to maintain reproducibility, agarose bead preparations were deemed acceptable if the CFU concentration, the bead volume per milliliter, and the bead size were all consistent.

Infection

P. aeruginosa-laden agarose beads were administered at a concentration of 1×10^6 CFU/mL, via oro-tracheal administration. Rats were anesthetized using isoflurane and suspended on an intubation stand (Braintree Scientific) by their incisors. The tongue was pulled out and aside using blunt forceps and a syringe attached to a blunt 18-gauge Luer stub (Instech Laboratories, Plymouth Meeting, PA, USA) inserted past the tongue and into the trachea to ensure delivery to the lung. 300 µL of the beads were delivered via syringe for an inoculum of 3×10^6 CFU, followed by 50 µL of air. Rats remained upright on the intubation stand for $\geq$5 s to complete inhalation of the inoculum and then were allowed to recover. Rats were weighed before the experiment began (day 0) and daily until sacrifice for the duration of the study.

Bronchoalveolar lavage

Rats were euthanized via intraperitoneal injection of 500 µL pentobarbital sodium (390 mg/mL). Rats were exsanguinated, the thoracic cavity exposed, and airways intubated via the lower trachea. 5 ml of sterile, cold PBS pushed into the lungs and recollected into a separate sterile syringe using a two-way stopcock. Bronchoalveolar lavage fluid (BALF) was centrifuged at 1200 rpm for 7 min, and the supernatant transferred for mucin analysis. Pelleted cells were resuspended in PBS and cytocentrifuged onto slides at 500×*g* for 5 min. Slides were fixed and stained with Diff-Quik (Siemens, Erlanger, Germany). Leukocytes were manually counted and visually identified.

CFUs

Lungs were mechanically homogenized in 5 mL of F-12 media (Gibco, Thermofisher Scientific, Grand Island, NY, USA) and 200 µL aliquots serially diluted in TSB for manual counting on Pseudomonas Isolation Agar (Millipore Sigma, St. Louis, MO, USA).

Histology

Tracheae and lungs were immersion fixed in 10% phosphate-buffered formalin and embedded in paraffin blocks for sectioning, as previously performed [28]. Sections were stained with hematoxylin and eosin (H&E) or alcian blue Periodic acid Schiffs (ABPAS).

Mucin analysis

Muc5b and Muc5ac were detected on nitrocellulose membranes using modified dot blot methods [25] and antibodies selective for each mucin (Muc5b ab87376 Abcam, Cambridge, MA, United States; Muc5ac 10112-334, VWR, Radnor, PA, United States), as previously performed [24]. Signal was detected with HRP-secondary antibodies and the SuperSignal West Femto Maximum Sensitivity Substrate (Thermofisher Scientific, Grand Island, NY, United States). Blots were detected for chemiluminescence and analyzed by densitometry using ImageJ software. Samples were normalized to age-matched WT control average values.

Tracheal short-circuit current

Short-circuit current measurements were performed as described in previous studies under voltage clamp conditions in Ussing chambers (Physiologic Instruments, Reno, NV, USA) [28]. Briefly, tracheae were excised and opened longitudinally along the ventral surface. Tracheal tissues were mounted as flat sheets in Ussing chambers (area 0.031 cm^2). Chambers were constantly maintained at 37 °C and bubbled vigorously with 95% O_2:5% CO_2. Tissue segments were equilibrated for 10 min in regular Ringer solution that contained (in mM) 120 NaCl, 25 $NaHCO_3$, 3.33 KH_2PO_4, 0.83 K_2HPO_4, 1.2 $CaCl_2$, 1.2 $MgCl_2$, and 10 mannitol to establish a baseline. This was followed by administration of $CFTR_{Inh\text{-}172}$ (10 µM) to block constitutively active CFTR-dependent chloride current, and then sequential addition of amiloride (100 µM), ATP (10 µM), and bumetanide (100 µM). I_{sc} divergence was calculated after subsequent attainment of stable plateau after baseline and CFTR inhibitor treatment for several minutes for each sample.

µOCT image acquisition and analysis

Functional microanatomic measurements of ex vivo tissue were performed using micro-optical coherence tomography [23, 30, 31], as described previously. Trachea were excised and images were acquired at five controlled points along the ventral surface with the optical beam scanned along the longitudinal direction, using the cranial end as a reference. Mucociliary transport (MCT) rate was determined using time elapsed and distance travelled of native particulates in the mucus over multiple frames, using the pixel to micron conversion factor determined with image calibration.

Statistics

Statistical analysis was performed in GraphPad Prism (GraphPad, LaJolla, CA) version 7.0 or newer. Inferential statistics (mean, SD, and SEM) were computed using ANOVA or 2-tailed paired t-test, as appropriate. For multiple comparisons, post-hoc testing was applied only if ANOVA was significant. P values of less than 0.05 were considered significant. Statistics are presented as mean ± SEM. For all analyses, mean values per animal are reported.

Study approvals

Procedures involving animals were approved by the IACUC at UAB (IACUC-20532, IACUC-21963, and IACUC-22206).

Results

Ivacaftor treatment has transient effects on infectious burden in the hG551D rats

Our initial studies were designed to mimic the scenario that many PwCF face when initiating HEMT, which is prior infection with pathogens like *P. aeruginosa*. In these experiments, we infected hG551D and WT rats with 3×10^6 CFUs of the mucoid clinical isolate PAM57-15, embedded in agarose beads. To mimic an acute course of infection with HEMT, infected rats received either ivacaftor or methylcellulose vehicle daily for 3 days (Fig. 1A) beginning at day 4 post-infection, while ivacaftor treatment was delayed until 21 days after infection to mimic the chronic infection. At sacrifice, hG551D rats in the acute cohort had a lower bacterial burden in the lung, measured by fewer CFUs recovered, when the treatment was ivacaftor ($1.1\times10^5\pm1.3\times10^5$ CFUs compared to the vehicle only (5.3×10^5 CFUs $\pm 2.0\times10^5$ CFUs, Fig. 1B). However, the hG551D rats in the chronic cohort had no difference in CFUs after sacrifice regardless of treatment group ($2.9\times10^5\pm1.5\times10^5$ CFUs in the ivacaftor group compared to $2.2\times10^5\pm4.1\times10^5$ CFUs in the control). In each case, the WT rats were able to eradicate infection, as previously seen [24]. Neutrophil infiltration was assessed as a marker of inflammation. Treatment with ivacaftor did not reduce the number of neutrophils compared to the vehicle group at either day 7 (59.7% ± 10.23% in the ivacaftor group compared to 67.9% ± 8.2% in the control) or day 39 (27.9% ± 13.5% in the ivacaftor group compared to 17.1% ± 12.7% in the vehicle group), and both hG551D groups had higher percentage than WT (58.7% ± 10.8% at day 7, and 3.2% ± 2.9% at day 28, Fig. 1C), as previously reported [22, 24].

In the acute cohort, hG551D rats that were treated with ivacaftor had a significant increase in weight 24 h after treatment initiation compared to the vehicle only group of hG551D rats (Fig. 1D), and ended with the largest change from the initial weight of all three groups. Similarly, the hG551D rats in the chronic cohort had a significant weight increase 24 h after the initial treatment, continuing to gain compared to the vehicle only group (Fig. 1E), although the weights had not reached the gain status of the WT group by the end of the study. We also measured mucin content in the BALF, as this response to infection marked the severity of disease in the previous CF rat studies [24, 25]. The hG551D rats had no statistical difference between the groups in Muc5b, either at the acute or the chronic timepoint (Fig. 1F), although both groups were markedly higher than WT. Ivacaftor treatment did reduce Muc5ac in the hG551D rats at the acute timepoint, although there was no difference at the chronic timepoint in Muc5ac between the ivacaftor and the vehicle groups (Fig. 1G).

Preventive treatment with ivacaftor ameliorates acute, but not chronic, infection outcomes

Although the differences between the treatment groups were minimal when bacterial infection preceded ivacaftor therapy, we also asked if ivacaftor could preventively alter the response to bacterial infection. This experiment addressed the situation that more pwCF will face in the future, as the FDA has now approved ivacaftor therapy down to 1 month of age [11]. Therefore, newly diagnosed pwCF will have CFTR modulator correction before exposure to bacteria such as *P. aeruginosa*. To test how ivacaftor would modulate the response to infection in this clinical scenario, we initiated treatment for all groups of hG551D rats at Day −7 (Fig. 2A), with rats evenly split into ivacaftor and vehicle only groups, again compared to WT. Rats were infected with *P. aeruginosa* as before at day 0, when the drug concentrations could be expected to be at steady-state. In this experiment, we again found decreased lung burden, assessed by CFUs, in the ivacaftor-treated hG551D group at the acute timepoints, days 3 ($1.9\times10^2\pm1.6\times10^2$ CFUs in the ivacaftor group compared to $4.9\times10^5\pm1.6\times10^4$ CFUs in the vehicle group) and 7 ($2.8\times10^1\pm19.8\times10^1$ CFUs in the ivacaftor group compared to $6.3\times10^3\pm3.7\times10^3$ CFUs in the vehicle group), but had returned to match the vehicle only group by day 28 post-infection ($1.3\times10^7\pm1.7\times10^5$ CFUs in the ivacaftor group compared to $1.5\times10^7\pm1.6\times10^5$ CFUs in the vehicle group, Fig. 2B). Similarly, the percentage of cells in the BALF that were neutrophils were significantly lower in the ivacaftor-treated hG551D rats (25.1% ± 23.8%) compared to both the vehicle only hG551D rats (74.8% ± 16.5%) and the WT controls (64.2% ± 12.2%) at day 3, but had returned to match the vehicle only group at day 28 (29.3% ± 19.1% in the ivacaftor group, compared to 26.83% ± 15.1% in the vehicle group, Fig. 2C). Again, weights were recorded from the day of infection, finding that the hG551D rats treated with ivacaftor had significantly higher weight gains compared to both the vehicle-hG551D and the WT control groups (Fig. 2D). In this experiment, there was no difference between the two hG551D treatment groups in the amount of Muc5b in the BALF at days 3 and 7 post-infection, although there was a higher amount of Muc5b in the BALF in the ivacaftor rats at day 28 (Fig. 2E). Similarly, Muc5ac was not different between the two hG551D treatment

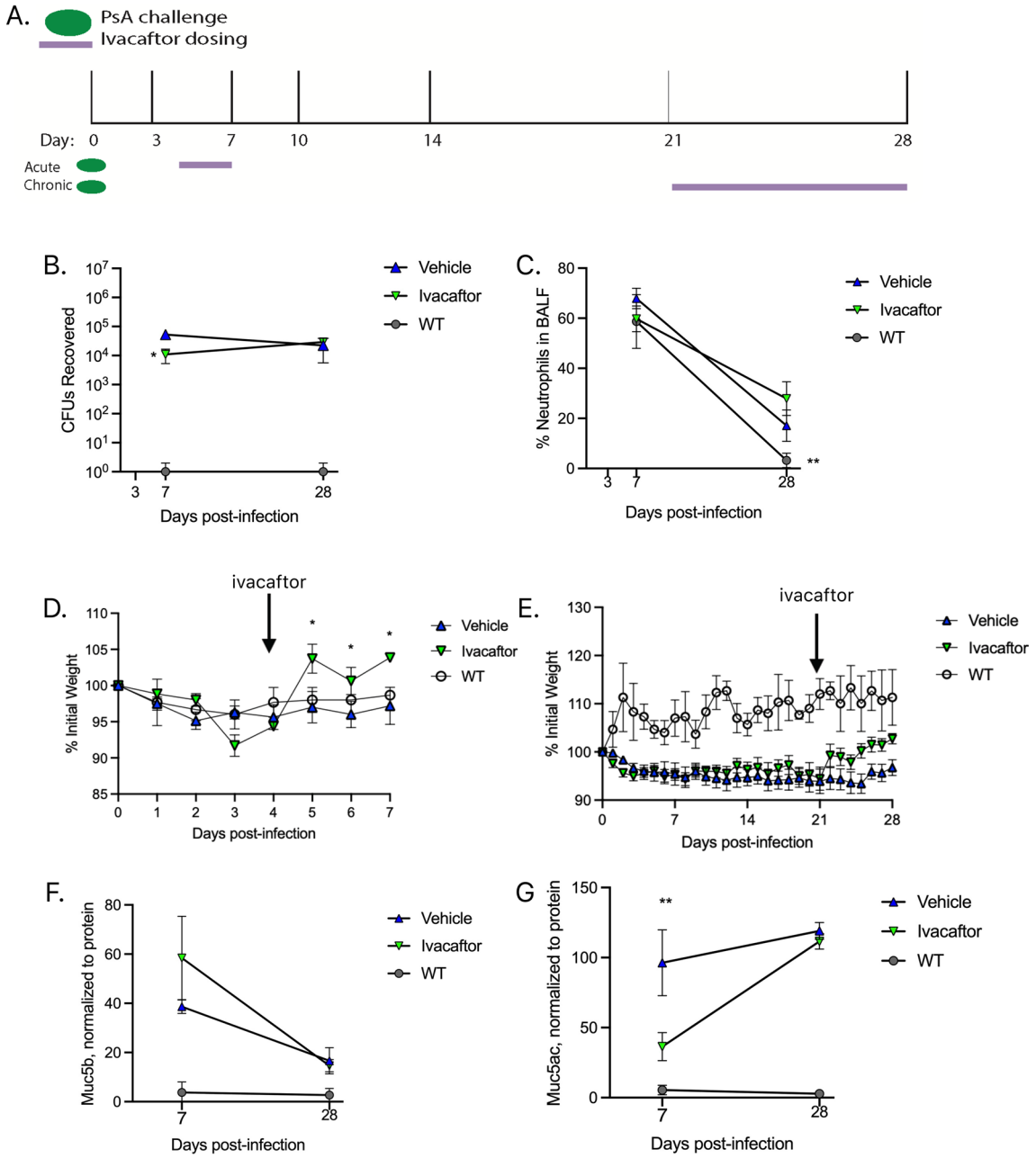

Fig. 1 Treatment with ivacaftor reduces acute, but not chronic, *P. aeruginosa* lung burden. **A** Experimental diagram. Rats were infected with *P. aeruginosa* at day 0, and ivacaftor dosing initiated at either day 4, during the acute phase, or day 21, during the chronic phase. Rats were sacrificed at either day 7 or 28 post-infection. **B** CFUs recovered from the lung homogenate of a single lung lobe. **C** Percentage of neutrophils from the differential cell count in the bronchoalveolar lavage fluid. **D** Weight change from baseline, in percent, in the acute cohort. **E** Weight change from baseline in the chronic cohort. **F** Muc5b quantity and **G** Muc5ac quantity detected in the BALF. Circles = WT rats; blue upward triangles = hG551D + vehicle; green downward triangles = hG551D + ivacaftor. Arrows indicate initiation of ivacaftor therapy. Data reported as mean ± SD. n = 6/group. *P < 0.05, **P < 0.01

groups at the early timepoints, but higher in the ivacaftor-treated rats at the 28 day timepoint (Fig. 2F).

Potentiation of G551D-CFTR by ivacaftor results in similar activity to WT during infection

Although we have previously found that ivacaftor restores CFTR protein function to the airways of

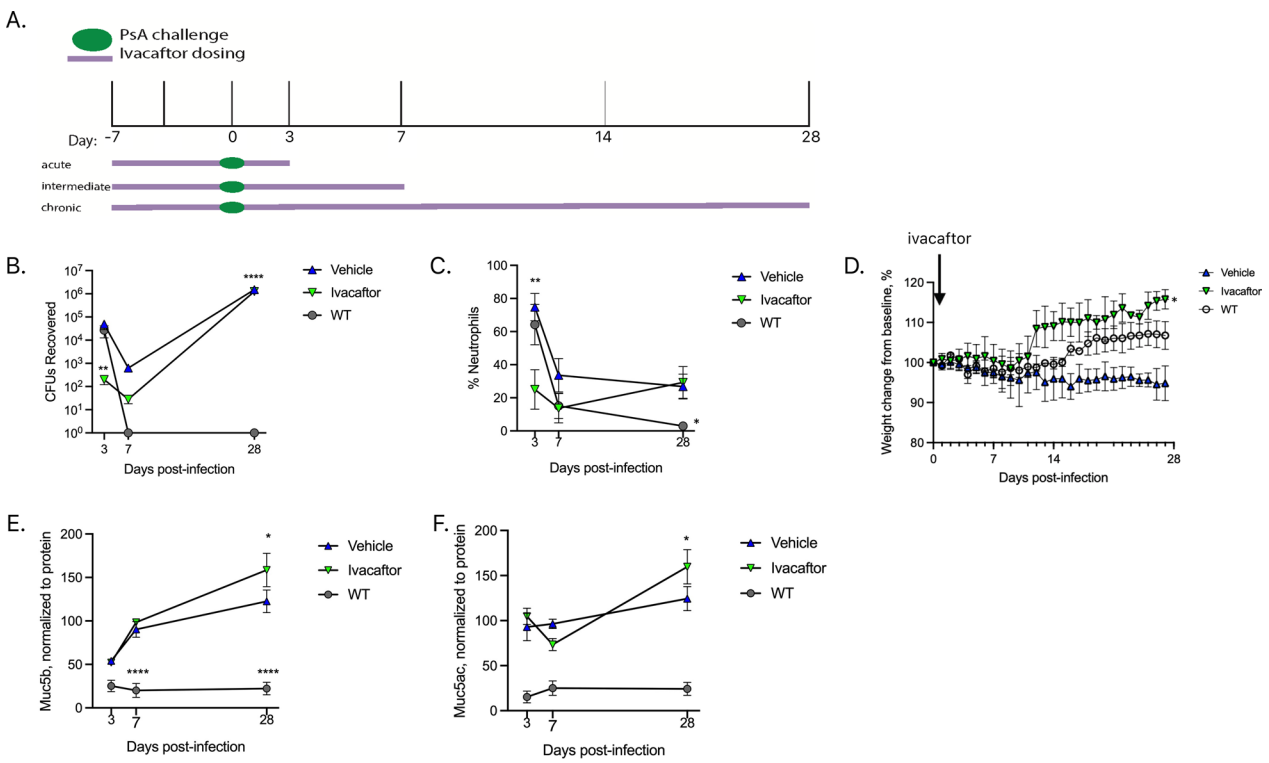

Fig. 2 Prevention of infection with ivacaftor reduces acute, but not chronic, *P. aeruginosa* lung burden. **A** Experimental diagram. Ivacaftor or vehicle treatment was initiated 7 days before infection with *P. aeruginosa* at day 0, and continued until the rats were sacrificed. during the acute phase, or day 21, during the chronic phase. Rats were sacrificed at day 3, 7, or 28 post-infection. **B** CFUs recovered from the lung homogenate of a single lung lobe. **C** Percentage of neutrophils from the differential cell count in the bronchoalveolar lavage fluid. **D** Weight change from baseline, in percent. **E** Muc5b quantity and **F** Muc5ac quantity detected in the BALF. Circles = WT rats; blue upward triangles = hG551D + vehicle; green downward triangles = hG551D + ivacaftor. Arrows indicate initiation of ivacaftor therapy. Data reported as mean ± SD. n = 6/group. *P < 0.05, **P < 0.01, ****P < 0.0001

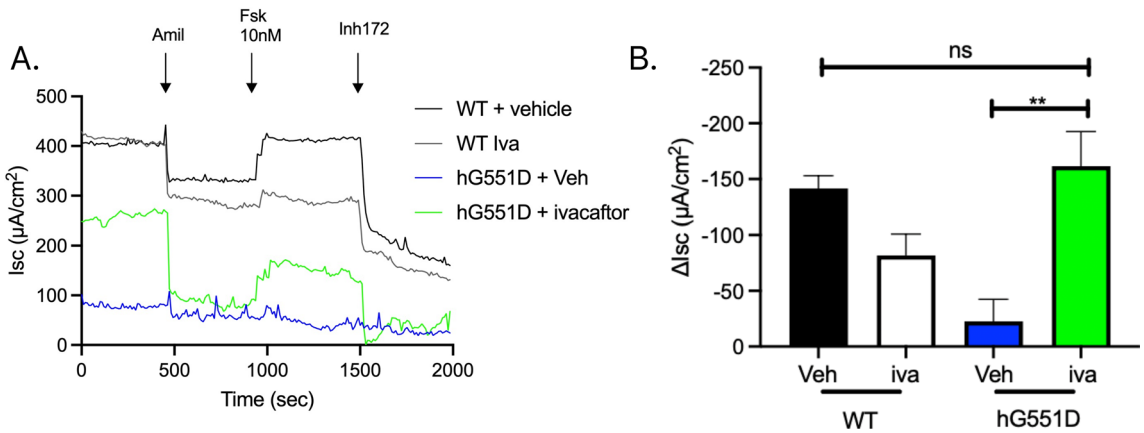

Fig. 3 Ivacaftor potentiation of G551D-CFTR improved during chronic infection. Ivacaftor or vehicle treatment was initiated 7 days before infection with *P. aeruginosa* at day 0, and continued until the rats were sacrificed at 28 days post-infection. Tracheae were excised for short-circuit current analysis. **A** Representative tracings of each group. Arrows indicate the time that amiloride, forskolin, or CFTR-$_{Inh172}$ was added. **B** Summary change in I_{sc} after addition of CFTR-$_{Inh172}$ for each group. Data reported as mean ± SD. n = 6/group. **P < 0.01

hG551D rats [21], it is not clearly understood how the efficacy of CFTR correction changes after infection, or if WT CFTR function is altered during infection. To assess this question, we treated both WT and hG551D rats with either ivacaftor or the vehicle, and infected all rats for 28 days. The CFTR activity in the trachea was assessed using short-circuit current measurements. Representative tracings from all four groups are shown for comparison (Fig. 3A). The baseline current in the WT rat tracheae was not affected by ivacaftor treatment, although the changes following forksokin and CFTR-$_{Inh}$172 administration were lower in the WT that received ivacaftor compared to the vehicle control. As expected, ivacaftor treated hG551D rats had a higher baseline current compared to the vehicle treated hG551D rats, which reached approximately 50% of WT, which matches the effect of ivacaftor in uninfected hG551D rats that we have previously reported [21]. To assess CFTR-dependent current, we assessed the change in I_{sc} after administration of CFTR-$_{Inh}$172, comparing the vehicle and ivacaftor treated groups. The mean response to CFTR-$_{Inh}$172 was not significantly different in the ivacaftor treated WT group (-81.7 ± 33.2 μA/cm^2) compared to vehicle control (-141.6 ± 16.19 μA/cm^2). The vehicle treated hG551D rats had a reduced response compared to WT (-22.5 ± 44.6 μA/cm^2), as expected. There was no decrement to the CFTR-dependent current in the hG551D rats treated with ivacaftor (-161.5 ± 62.3 μA/cm^2) even with infection; this was significantly higher than the hG551D vehicle controls, and no different compared to the WT groups. These data indicated that there was no difference in CFTR protein function in the hG551D-ivacaftor corrected animals, even with infection.

Ivacaftor treatment reduces the mucus burden during infection

Previous work conducted in the rat models have carefully characterized airway mucus the CF airway, at baseline and in response to infection with *P. aeruginosa*. Prior work has identified a deficit in mucociliary transport in the CF airway [23], that is exacerbated by infection [24]. In the absence of infection, the administration of ivacaftor has been shown to correct the mucociliary transport defect [21], corroborating data obtained by other groups [32]. We wanted to confirm that the correction of MCT rate in the hG551D trachea with ivacaftor was sustained in the presence of infection. To determine this, we again treated hG551D rats with either ivacaftor or vehicle control, and assayed rats in the acute (day 3) and chronic (day 28) phases of infection. The airway was imaged with μOCT to capture the airway surface. Representative images are presented of tracheae from hG551D rats in the acute and chronic phases, treated with either vehicle or ivacaftor (Fig. 4A). These images were used to quantitate changes to the airway surface liquid (ASL) height as well as MCT rates. At the acute timepoint, we found that infection with *P. aeruginosa* increased ASL height in the WT rats (40.6 ± 12.6 μm with *P. aeruginosa* compared to 21.5 ± 13.4 in the uninfected WT), but that infected hG551D rats treated only with the vehicle had a significantly reduced ASL (22.7 ± 5.6 μm). Ivacaftor did not restore ASL height in the hG551D rats that were infected with *P. aeruginosa* (14.2 ± 9.2 μm, Fig. 4B).

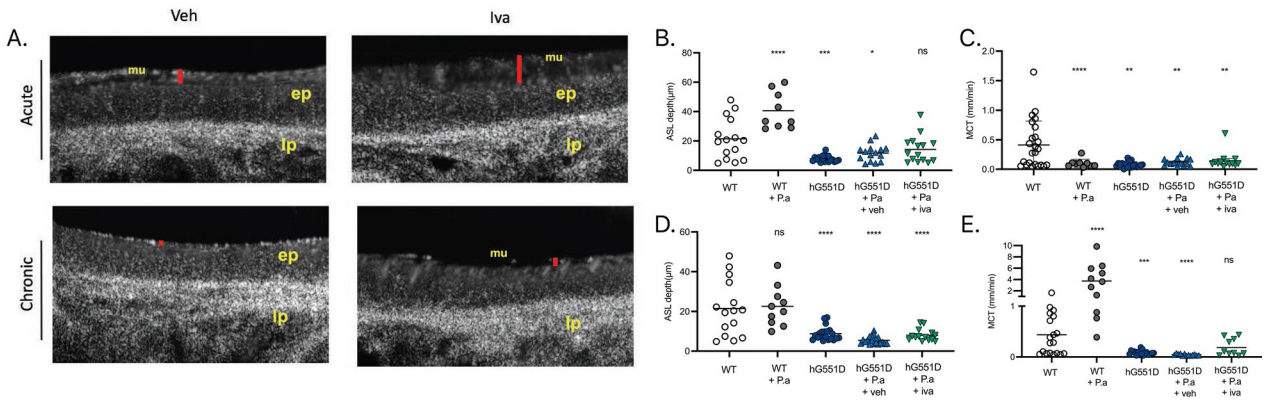

Fig. 4 Ivacaftor corrects mucociliary transport in chronic infection. Ivacaftor or vehicle treatment was initiated 7 days before infection with *P. aeruginosa* at day 0, and continued until the rats were sacrificed at 3 or 28 days post-infection. Tracheae were excised for μOCT imaging. **A** Representative tracings of hG551D trachea with vehicle (veh) or ivacaftor (iva), during acute (3 days post-infection) or chronic infection (28 days post-infection). Red bar = airway surface liquid (ASL) depth, mu = mucus layer, ep = epithelial layer, and lp = lamina propria. Images were quantified to generate, **B** ASL depth and **C** mucociliary transport (MCT) rates in acute infection, as well as **D** ASL depth and **E** MCT rates from chronic infection. Data reported as mean, and all graphs have statistical comparisons for each group to the uninfected WT (open circles). n = 15 RO1/group. *P < 0.05, **P < 0.01, ***P < 0.001, ****P < 0.0001, ns = not significant

However, at the acute timepoint, when compared to MCT rates detected in the WT uninfected tracheae (0.42 ± 0.07 mm/min) ivacaftor did not restore MCT (0.14 ± 0.14 mm/min), which was also non-significant compared to the hG551D uninfected (0.07 ± 0.04 mm/min) and the hG551D rats that were infected and treated only with vehicle (0.12 ± 0.06 mm/min, Fig. 4B). The same analysis was conducted at the chronic infection timepoint. In these animals, ivacaftor did not restore ASL to that of WT in the hG551D infected rats (8.09 ± 3.04 µm hG551D + ivacaftor, compared to 21.45 ± 13.9 µm in the uninfected WT, Fig. 4D). MCT rates in the tracheae from the infected hG551D rats treated with ivacaftor (0.19 ± 0.17 mm/min) were higher than the infected hG551D rats treated only with vehicle (0.04 ± 0.017 mm/min, Fig. 4E). Importantly, the WT rats that were infected with *P. aeruginosa* had a significantly increased mean MCT rate (3.7 ± 2.9 mm/min), which corresponds with data previously reported [24]. The difference between the infected WT and the infected hG551D + ivacaftor is a potential mechanism for retention of infection.

We have previously found that infection with *P. aeruginosa* caused small airway plugging at the chronic timepoint in CF rats [24]. That data was repeated in the hG551D rats that were infected and treated only with vehicle (Fig. 5A), which had significant mucus plugging in the small airways at both the acute and the chronic timepoints. These plugs appeared to be less severe in the ivacaftor treated hG551D rats at the acute timepoint, and largely absent at the chronic timepoint (Fig. 5A). To quantify these changes, we measured the percent of total airways that had mucus staining present in the airway lumen (Fig. 5B), which identified a statistically significant difference only in the ivacaftor treated hG551D rats at the chronic timepoint (2.7 ± 3.9% affected airways in the ivacaftor treated hG551D compared to 36.5 ± 13.1%in the control). For the airways that had mucus present, we measured the percent of the airway that was occluded (Fig. 5C), which indicated statistically significant differences in the ivacaftor treated rats at both the acute (33.5 ± 14.8% in the ivacaftor treated hG551D compared to 57.5 ± 26.9% in the vehicle treated hG551D) and the chronic (2.08 ± 3.5% in the ivacaftor treated hG551D compared to 50.3 ± 24.4% in the vehicle treated) timepoints. Together, these data indicate that the mucus phenotype in response to infection is ameliorated but not eradicated in the hG551D rats with restored CFTR function.

Discussion

Overall, our data found that ivacaftor administration resulted in slightly ameliorated infectious burden in the acute phase, but was unable to significantly clear infection once *P. aeruginosa* had reached chronicity. These data match results from the observational clinical trial including people with the G551D mutation on ivacaftor, termed GOAL [19]. In this study, researchers found that pwCF had short-term reductions in inflammation and bacterial burden, with additional conversion of mucoid *P. aeruginosa* to non-mucoid *P. aeruginosa*. However, once patients had been on ivacaftor therapy for a full year, markers of inflammation and infection had returned to baseline [20]. Our rat data also correlates to the improvement in whole-lung mucociliary clearance seen in those on ivacaftor [16], which in humans corresponds to a significant reduction in expectorated sputum.

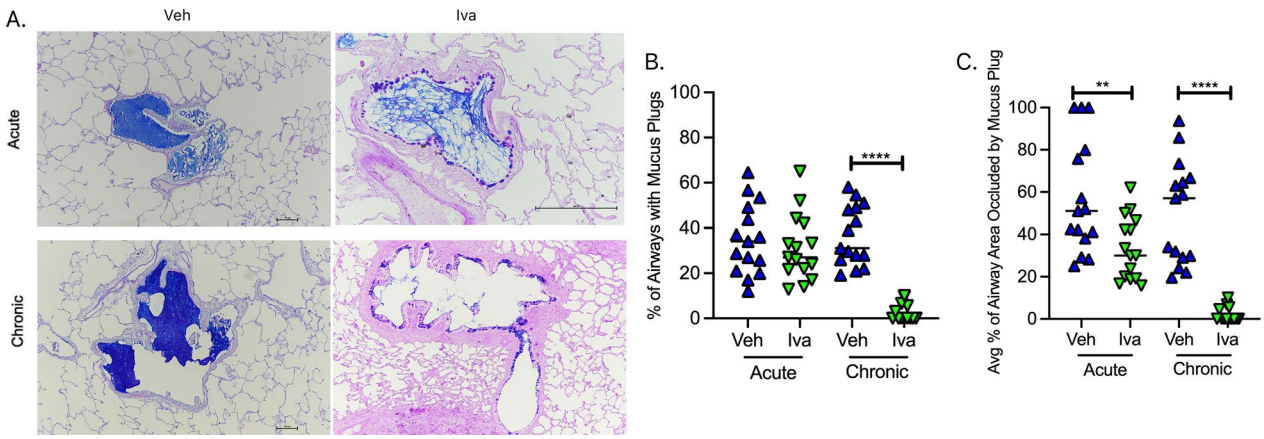

Fig. 5 Ivacaftor relieves mucus burden in acute and chronic infection. Ivacaftor or vehicle treatment was initiated 7 days before infection with *P. aeruginosa* at day 0, and continued until the rats were sacrificed at 3 or 28 days post-infection. Lung sections were stained for the presence of mucus using AB-PAS. **A** Representative tracings of hG551D trachea with vehicle (veh) or ivacaftor (iva), during acute or chronic infection. Images were quantified to generate **B** % of airways with mucus plugs. **C** Airways that had mucus present were further analyzed to determine the percentage of the airway that was occluded. Data are presented as mean. n = 15 RO1/group. **P < 0.01, ****P < 0.0001

More data has been available from the recent PROMISE study, which includes more pwCF on highly effective modulators. In this study, those eligible for elexacaftor/tezacaftor/ivacaftor (Trikafta), who were predominantly those with F508del mutations, demonstrated significant clinical improvement [10, 18] but residual bacterial burden [12]. This population experienced dramatic reduction in exacerbations, hospital visits, and antibiotic usage, but remained largely infected. With the human data in mind, we hypothesize that the mucus occlusions caused more of the symptoms than the overall lung burden. This is supported by the data presented here, that the rat weights are significantly improved with ivacaftor treatment, even when bacteria are still in high numbers. Instead, the improved weights of the hG551D rats treated with ivacaftor correlated more closely to the absence of accumulative mucus in the airways. In pwCF, bacterial burden does not always match the clinical course of disease, which is most clearly seen by the lack of increased bacterial density in exacerbations. Additionally, the strongest effect of ivacaftor in the infected hG551D rats came in the acute phase of the infection, which correlates more closely to the exacerbations experienced by pwCF.

Reduction of exacerbations with administration of HEMT may be more dependent on the localization of infection. In these experiments, we found that although the ivacaftor-treated hG551D rats no longer had widespread areas of mucus plugs, there were some airways that remained filled with mucus during chronic infection. The localized affected airways may have implications for more severe lung disease. The presence of bronchiectatic airways are expected to be more difficult to eradicate with administration of HEMT, and may continue to provide a reservoir for infection. This will become especially important in the case of a lapse in therapy, which has already been shown to result in renewed exacerbation [33]. These regions should also be taken into consideration as the field moves toward lung delivery of CFTR genetic therapies. Restoration of CFTR activity may not completely resolve all areas of lung infection and mucus accumulation, as seen in these experiments.

Importantly, we also found that the ivacaftor-treated rats have improved global outcomes, with increased weights, increased CFTR activity, and decreased mucus accumulations, even in the setting of chronic infections. These suggest that the presence of infection has been decoupled from the mucus and CFTR function. These data also suggest that the primary morbidity in the infected CF rats results from plugged airways that are not able to conduct oxygen, which may also explain why pwCF have significantly improved BMI and quality of life, even with reports of continued bacterial colonization. Additionally, these data suggest that HEMT may improve tolerance of bacterial infections, therefore improving patient outcomes.

It is clear from both the human data reports and the animal experiments presented here that HEMT does not eradicate infection alone. What is less clear for this population is whether the residual bacteria will cause a significant decline in lung health. Longer-term studies will be needed to determine if lung function continues to decline on HEMT, even if more slowly than before the HEMT era, or if the residual bacteria become more clinically significant during a viral exacerbation. Based on the similarities to the human results, we believe that the hG551D rat can be a suitable model for prediction of these events, and future studies will attempt to understand how lung health has changed in the HEMT era.

Acknowledgements
The authors also acknowledge the assistance of Dezhi Wang and the Histomorphometry and Molecular Analysis Core.

Author contributions
SEB conceived of the experiments; JDK, MMT, GB, AMO, IHD, and SEB performed the experiments and analyzed the data; SEB contributed reagents, materials, and analysis tools, and supervised the project; JDK, MMT, GEB, and SEB wrote the manuscript.

Funding
This work was supported by the National Heart, Lung, and Blood Institute [K08HL131867, R01HL153079], the National Institute of Diabetes, Digestive, and Kidney Diseases [P30DJ072482], and the Cystic Fibrosis Foundation [BIRKET-20A0KB].

Availability of data and materials
No datasets were generated or analysed during the current study.

Declarations

Ethics approval and consent to participate
Procedures involving animals were approved by the IACUC at UAB (IACUC-20532, IACUC-21963, and IACUC-22206).

Competing interests
The authors declare no competing interests.

Received: 6 September 2024 Accepted: 28 October 2024
Published online: 04 November 2024

References

1. Ramsey BW, et al. A CFTR potentiator in patients with cystic fibrosis and the G551D mutation. N Engl J Med. 2011;365(18):1663–72.
2. Van Goor F, et al. Rescue of CF airway epithelial cell function in vitro by a CFTR potentiator, VX-770. Proc Natl Acad Sci USA. 2009;106(44):18825–30.
3. Rowe SM, et al. Parallel effects of VX-770 on transepithelial potential difference in vitro and in vivo. J Cyst Fibros. 2010;9(Supplement):S20.
4. Van Goor F, et al. Correction of the F508del-CFTR protein processing defect in vitro by the investigational drug VX-809. Proc Natl Acad Sci USA. 2011;108(46):18843–8.
5. Yu H, et al. Ivacaftor potentiation of multiple CFTR channels with gating mutations. J Cyst Fibros. 2012;11(3):237–45.

6. Van Goor F, et al. Effect of ivacaftor on CFTR forms with missense mutations associated with defects in protein processing or function. J Cyst Fibros. 2013;13(1):29–36.
7. Davies JC, et al. VX-659-tezacaftor–ivacaftor in patients with cystic fibrosis and one or two Phe508del alleles. N Engl J Med. 2018;379(17):1599–611.
8. Keating D, et al. VX-445-tezacaftor–ivacaftor in patients with cystic fibrosis and one or two Phe508del alleles. N Engl J Med. 2018;379(17):1612–20.
9. Nichols DP, et al. PROMISE: working with the CF community to understand emerging clinical and research needs for those treated with highly effective CFTR modulator therapy. J Cyst Fibros. 2021;20(2):205–12.
10. Nichols DP, et al. Clinical effectiveness of elexacaftor/tezacftor/ivacaftor in people with cystic fibrosis. Am J Respir Crit Care Med. 2021;205(5):529–39.
11. Hisert KB, et al. Understanding and addressing the needs of people with cystic fibrosis in the era of CFTR modulator therapy. Lancet Respir Med. 2023;11(10):916–31.
12. Nichols DP, et al. Pharmacologic improvement of CFTR function rapidly decreases sputum pathogen density, but lung infections generally persist. J Clin Invest. 2023. https://doi.org/10.1172/JCI167957.
13. Accurso FJ, et al. Sweat chloride as a biomarker of CFTR activity: proof of concept and ivacaftor clinical trial data. J Cyst Fibros. 2014;13(2):139–47.
14. Fidler MC, et al. Correlation of sweat chloride and percent predicted FEV1 in cystic fibrosis patients treated with ivacaftor. J Cyst Fibros. 2017;16(1):41–4.
15. Rowe SM, et al. Clinical mechanism of the cystic fibrosis transmembrane conductance regulator potentiator ivacaftor in G551D-mediated cystic fibrosis. Am J Respir Crit Care Med. 2014;190(2):175–84.
16. Donaldson SH, et al. Effect of ivacaftor on mucociliary clearance and clinical outcomes in cystic fibrosis patients with G551D-CFTR. JCI Insight. 2018. https://doi.org/10.1172/jci.insight.122695.
17. Gabel ME, et al. Overweight and cystic fibrosis: an unexpected challenge. Pediatr Pulmonol. 2022;57(Suppl 1):S40–9.
18. Miller AC, et al. The rapid reduction of infection-related visits and antibiotic use among people with cystic fibrosis after starting elexacaftor–tezacaftor–ivacaftor. Clin Infect Dis. 2022;75(7):1115–22.
19. Heltshe SL, et al. Pseudomonas aeruginosa in cystic fibrosis patients with G551D-CFTR treated with ivacaftor. Clin Infect Dis. 2015;60(5):703–12.
20. Hisert KB, et al. Restoring cystic fibrosis transmembrane conductance regulator function reduces airway bacteria and inflammation in people with cystic fibrosis and chronic lung infections. Am J Respir Crit Care Med. 2017;195(12):1617–28.
21. Birket SE, et al. Ivacaftor reverses airway mucus abnormalities in a rat model harboring a humanized G551D-CFTR. Am J Respir Crit Care Med. 2020;202(9):1271–82.
22. Green M, et al. Ivacaftor partially corrects airway inflammation in a humanized G551D rat. Am J Physiol Lung Cell Mol Physiol. 2021;320(6):L1093–100.
23. Birket SE, et al. Development of an airway mucus defect in the cystic fibrosis rat. JCI Insight. 2018;3(1): e97199.
24. Henderson AG, et al. Static mucus impairs bacterial clearance and allows chronic infection with *Pseudomonas aeruginosa* in the cystic fibrosis rat. Eur Respir J. 2022;60(3):2101032.
25. Keith JD, et al. Muc5b contributes to mucus abnormality in rat models of cystic fibrosis. Front Physiol. 2022;13: 884166.
26. Rosen BH, et al. Infection is not required for mucoinflammatory lung disease in CFTR-knockout ferrets. Am J Respir Crit Care Med. 2018;197(10):1308–18.
27. Sun X, et al. In utero and postnatal VX-770 administration rescues multiorgan disease in a ferret model of cystic fibrosis. Sci Transl Med. 2019;11(485): eaau7531.
28. Tuggle KL, et al. Characterization of defects in ion transport and tissue development in cystic fibrosis transmembrane conductance regulator (CFTR)-knockout rats. PLoS ONE. 2014;9(3): e91253.
29. Cory TJ, et al. Impact of azithromycin treatment on macrophage gene expression in subjects with cystic fibrosis. J Cyst Fibros. 2014;13(2):164–71.
30. Liu L, et al. Method for quantitative study of airway functional microanatomy using micro-optical coherence tomography. PLoS ONE. 2013;8(1): e54473.
31. Birket SE, et al. A functional anatomic defect of the cystic fibrosis airway. Am J Respir Crit Care Med. 2014;190(4):421–32.
32. Morrison CB, et al. Treatment of cystic fibrosis airway cells with CFTR modulators reverses aberrant mucus properties via hydration. Eur Respir J. 2022;59(2):2100185.
33. Capraz Yavuz B, et al. Impact of interruption of CFTR modulator therapies. J Cyst Fibros. 2024;23(5):947–9.

Publisher's Note